Materials and Structures (2019) 52:1
https://doi.org/10.1617/s11527-018-1302-0

Biaxial bending of SFRC slabs: Is conventional reinforcement necessary?

Marco di Prisco · Matteo Colombo · Ali Pourzarabi

Received: 18 November 2018 / Accepted: 11 December 2018 / Published online: 22 December 2018

Abstract Fibre reinforced concrete shows enhanced performance in statistically redundant bi-dimensional structural elements that undergo biaxial bending. However, the lack of reinforcing rebars in fibre reinforced structural elements may affect the structural ductility which may further affect the overall load bearing capacity of these structures. To investigate the influence of fibres in such elements, six concrete plates of $2000 \times 2000 \times 150$ mm reinforced with steel fibres and/or reinforcing rebars are tested under a central concentrated load. Two of the elements are reinforced with only 35 kg/m^3 of steel fibres, two are reinforced with 2-way conventional reinforcing rebars (35 kg/m^3, in each direction) and two are reinforced with both steel fibres and rebars. The specimens are simply supported at the middle of each side by means of a bilateral restraint; the deflection response and cracking behaviour of all the specimens are recorded and compared. Moreover, the methodology introduced in the *fib* Model Code 2010 for design of steel fibre reinforced concrete is implemented to predict the ultimate load bearing capacity of these elements and its reliability is determined in comparison with the experimental values. The comparison of the behaviour of the specimens reinforced only with steel fibres, with those reinforced with steel rebars, shows the higher efficiency of steel fibres in terms of load carrying capacity, but with a lower ductility. The combination of steel fibres and rebars allows for a better exploitation of the capacity of both reinforcement solutions. Finally, the reliability of the approach implemented for the ultimate load prediction is shown and the need of rebars in providing ductility in fibre reinforced concrete members is underlined.

Keywords Biaxial bending · Reinforcement efficiency · Fibre reinforced concrete · Slabs · Serviceability and ultimate behaviour · Ductility

1 Introduction

The addition of steel fibres in concrete to prevent the brittle tensile behaviour shown by plain concrete has been studied for over half a century after the observation of the crack arrest mechanism by Romualdi and Batson [1]. As early as 1971, Shah and Rangan [2] pointed out the effect of fibres in tensile, flexural, and compressive behaviour of steel fibre reinforced concrete (SFRC) and also briefly studied some related aspects like fibre volume, geometry, and orientation on tensile behaviour of concrete. Ever since, different properties and influencing factors of this material have been extensively studied [3–6].

M. di Prisco (✉) · M. Colombo · A. Pourzarabi
Department of Civil and Environmental Engineering, Politecnico di Milano, Milan, Italy
e-mail: marco.diprisco@polimi.it

Steel fibres are commonly adopted as a substitution for diffused reinforcement in concrete structures. Fibre addition to reinforced concrete members is an effective solution for cracking control leading to more durable structures [7]. While in a conventionally reinforced concrete member tensile stresses are transferred to concrete between the cracks by stretched rebars through the steel–concrete bond, in fibre reinforced concrete (FRC), due to the presence of fibres, concrete is able to carry tensile stresses also along the cracks. This stiffening effect brought by fibres is responsible for closer crack spacing and narrower crack widths in a structural system containing both reinforcing bars and fibres (R/FRC) [8–12].

There are several studies in the literature concerning the simultaneous application of reinforcing bars and fibres in simply supported beams and slabs under a three-point or four-point bending test. Meda et al. [13] tested concrete beams of 2000 mm long in a four-point bending setup. The incorporation of 30 kg/m^3 and 60 kg/m^3 of steel fibres reduced deflections for respectively 7% and 25% in the SLS range of behaviour. Comparable results are reported by Oh [14] and Alsayed [15]. Vandewalle [16] studied the effect of fibre volume and aspect ratio on crack spacing in R/FRC beams and proposed a relationship to take into account the reduced crack spacing in these elements. The same testing method was adopted by Tan et al. [17] to examine short term and long term flexural cracking behaviour of R/FRC beams. A dosage of up to 2% of steel fibres with an interval of 0.5% volume was investigated in the beams. While primary cracks appeared at the location of stirrups, maximum crack width reduced with fibre dosage at all loading stages for an instantaneous deflection and also for long term flexural creep testing. Mertol et al. [18] tested lightly and heavily reinforced concrete beams with and without fibres and pointed out the effect of fibres in reducing ductility in very low reinforcement ratios. In a work by Pujadas et al. [19] concrete slabs of 3000 × 1000 × 200 mm were tested in a four-point bending configuration with addition of 0.25% and 0.5% by volume of steel and polypropylene fibres. Steel fibres were effective in both dosages in controlling crack widths, specifically in the serviceability range. Although the overall response in terms of load–deflection behaviour was comparable for all specimens, smaller deflections and higher load bearing capacities were obtained for specimens with fibres. Døssland [20] carried out three-point bending test under a concentrated load on R/FRC slabs of 3600 × 1200 mm. The R/FRC slabs containing 0.7% of fibres and a reinforcement ratio as low as $\rho_s = 0.07\%$ showed less deflection compared to the control specimen without fibres and having a $\rho_s = 0.33\%$. However, at a deflection of 20 mm a softening behaviour was observed for the R/FRC slabs.

Despite the advantages of application of steel fibres in reinforced concrete tension ties and statically determined structural elements under uniaxial bending, the highest advantages of this material would be in statically redundant structures in which stress redistribution may occur [21]. The greater number of yield lines needed for the formation of a failure mechanism, the higher would be the contribution of the fibres in the load carrying capacity of the structure [22]. Facconi et al. [23] investigated a thin slab of 4200 × 2500 × 80 mm which was once reinforced with 91 kg/m^3 of rebars and once with an optimized combination of 43 kg/m^3 of rebars and 25 kg/m^3 of steel fibres (in total 68 kg/m^3). There was an opening in the slab and it was continuously supported on all sides. While the R/C slab suffered from a sudden decay of stiffness after cracking, the R/FRC slab maintained its stiffness up to a much higher load and at collapse, smaller crack widths and higher maximum load were achieved for this specimen. Fall et al. [24] tested octagonal slabs with the reinforcement ratio being different in the two directions to create a weaker side in the slabs. The addition of 35 kg/m^3 of steel fibres reduced the deflection of the slabs under loading and the presence of fibres led to a more uniform load transfer at the position of the supports through a smearing effect.

The importance of structural indeterminacy in fibre reinforced structures is reflected in the *fib* Model Code 2010 (MC 2010) [25] where the use of fibres as sole reinforcement is permitted only if a certain level of ductility is provided to structural elements. In this regard two-way slabs are of particular interest as they may allow a significant stress redistribution when properly reinforced. This may explain why steel fibres have been extensively adopted in construction of flat slabs, slabs on pile, and slab on ground. Higher flexural strength and much higher ductility has been reported for FRC slabs on grade as compared to similar concrete slabs made of plain concrete [26–28].

Slabs on pile and elevated slabs have been successfully built and tested with only steel fibres with a dosage in the range of 45 kg/m^3 and 100 kg/m^3 [29, 30] for industrial, commercial, and residential buildings, with the presence of continuous steel rebars for connecting columns. To check the structural behaviour of SFRC slabs without any longitudinal reinforcement, an elevated flat slab with 9 bays built on 16 circular columns with a 6 m span for each panel and a thickness of 200 mm, reinforced only with 70 kg/m^3 of steel fibres (60 mm long and with a diameter of 1 mm) was tested in Limelette (Belgium) both in SLS and ULS conditions [31, 32]. A fully plastic behaviour was observed at the maximum load which occurred at a load higher than the prediction. However, the results raised some doubts about the overall ductility of the structure.

Despite all efforts devoted to better understand the structural behaviour of SFRC members, there is still a lack of experimental evidence on the behaviour of this material in statically redundant structural configurations. Therefore, an experimental programme is designed to investigate structural benefits and limitations of SFRC. In this paper, six concrete slabs supported at the middle of each side are tested under a biaxial bending condition. Two of the specimens are only reinforced with 35 kg/m^3 of steel fibres, two are reinforced with 35 kg/m^3 of reinforcing bars in each direction, and two are reinforced with the combination of both the two reinforcing solutions. Specifically, this work is aimed at investigating:

- the effectiveness of steel fibres versus reinforcing bars in terms of load bearing capacity;
- the ductility of SFRC slabs, particularly with reference to that required to activate the resistant mechanisms usually considered for R/C bi-dimensional elements according to limit analysis;
- to what extent the limited ductility of SFRC material may affect the overall structural response of a R/FRC element in biaxial bending.

To achieve these aims, measurements were carried out on the deflection and cracking behaviour of the slabs and comparisons were made based on test results. Furthermore, a yield line approach was adopted to estimate the ultimate bearing capacity and the results are compared with the experimental maximum loads.

2 Experimental programme

The experimental programme reported herein is part of a more extensive experimental campaign activated during the construction of the first industrial building in Italy, characterized by three different SFRC slab types: a foundation slab on piles (1436 m^2), two elevated solid slabs in R/FRC (540 m^2) and a partially prefabricated R/FRC slab supported on prestressed FRC beams (1171 m^2) [33]. Together with the six 2000 × 2000 × 150 mm concrete slabs reinforced with steel fibres and/or steel reinforcing bars tested under a central point load, six cubes and fourteen standard notched specimens were tested respectively in uniaxial compression and in a three-point bending setup (according to EN 14651 [34]) for material characterization. The test setup and a general scheme of the slab specimen is shown in Fig. 1.

2.1 Materials and specimen preparation

2.1.1 Materials

The concrete used in the present investigation is self-compacting with a mean compressive strength of 58 MPa determined on six cubes with a side of 150 mm. Its composition consists of 380 kg/m^3 of CEM IV 42.5R and 100 kg/m^3 of calcium carbonate filler. The water/binder ratio is 0.36 and 1.2% by weight of cement of superplasticizer is added. The mixture contains 0/4 sand, 0/8 sand and 8/14 gravel in dosages of 450 kg/m^3, 850 kg/m^3, and 425 kg/m^3 respectively. The same mixture was used to produce both the plain concrete and the SFRC: in the latter 35 kg/m^3 of double hooked-end steel fibres were added. The steel fibres used were 60 mm long with a diameter of 0.9 mm. According to the manufacturer, the tensile strength is 1500 MPa and the Young's modulus is 210 GPa.

The properties of the steel rebars were assessed testing four specimens. The average yield and ultimate strengths of the reinforcing steel were found to be 527 MPa and 647 MPa, respectively. The average ultimate strain obtained from the four specimens was 18.75%. Figure 2 shows the nominal stress–strain curves obtained for the specimens.

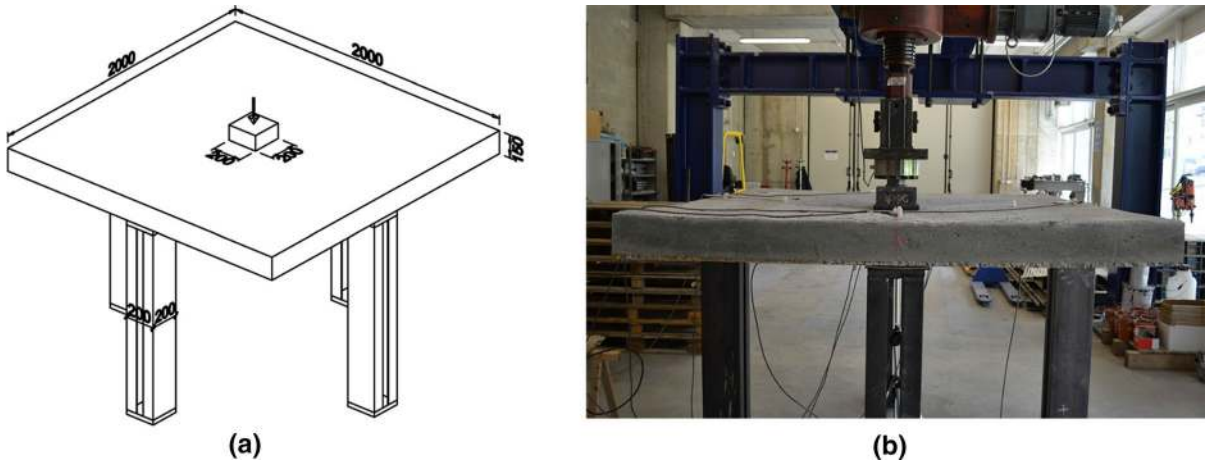

Fig. 1 **a** Sketch of the experimental setup; **b** an image of a loaded slab

2.1.2 Specimen preparation

As stated in the introduction, two slabs were reinforced only with steel fibres (SFRC1, SFRC2), two were cast with plain concrete and reinforced with 35 kg/m^3 of rebars in each direction (12Φ 12 mm rebars equally spaced in both directions) (R/C1, R/C2), and in the last two ones steel fibres and rebars were combined (R/FRC1, R/FRC2). In the specimens the rebars were placed at the bottom with a minimum cover of 30 mm from each side. During casting, the concrete was pumped from a truck mixer to the centre of the formworks to allow a radial flow of the fresh concrete and no vibration was carried out. It has been shown that fibres tend to align perpendicularly to the flow direction in concrete slabs [35–38] which increases the fibre effectiveness [39]. After casting, all specimens were covered with wet burlaps and kept moist for a couple of days. Then, they were kept in atmospheric condition until the day of testing. The 600 × 150 × 150 mm prismatic beams were cast together with the slabs and were notched at the mid-span to a depth of 25 mm. The six cubes were cured 35 days in the conditioning room in the lab at 20 °C and RH 90% and then tested.

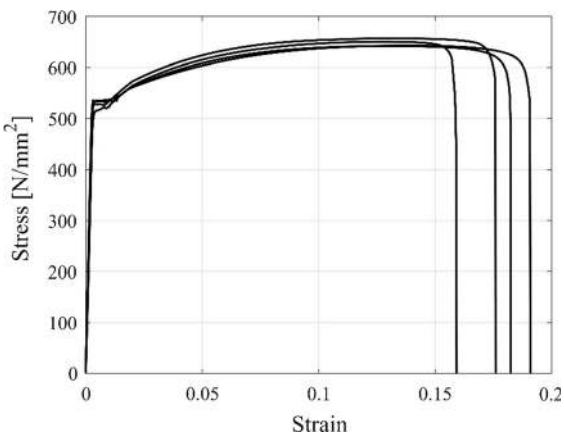

Fig. 2 Uniaxial tension test on rebars

2.2 Bending test on notched beams

The tests were carried out according to EN14651 [34] controlling the Crack Mouth Opening Displacement (CMOD) that was measured by a clip gauge introduced between two aluminium supports glued at the tip of the notch. According to the MC 2010, characterization of the post-peak residual strength of FRC in a three-point bending test is achieved by considering the residual flexural tensile strength, $f_{R,i}$ i = 1:4, at CMOD$_i$ = 0.5, 1.5, 2.5, and 3.5 mm. From the fourteen specimens, 5 were tested at 34 days of age, 5 were tested with the first SFRC slab test at 167 days, and 4 specimens were tested at the end of the complete experimental campaign at 220 days.

2.3 Slab tests

2.3.1 Loading and support conditions

The load was applied in the centre of the specimens by means of an electro-mechanical jack with a maximum

capacity of 1000 kN by adopting a displacement control procedure. A constant displacement rate equal to 20 μm/s was imposed to the steel loading head characterized by a cross section of 200 × 200 mm. A neoprene sheet of 220 × 220 × 30 mm was placed under the loading point. The slabs were supported at the middle of each side. The supports consist of two UNP 200 profiles that were placed 50 mm apart and were welded on a top and bottom steel plate with dimensions of 200 × 200 × 30 mm. A 5 mm thick neoprene sheet was placed between the specimen and the support. There was a hole on the support top plate to facilitate the insertion of a M16 bolt that was screwed in a threaded fixing anchor device embedded in the specimens to create a bilateral support. The length of the anchorage device was 100 mm, with a threaded length of 62 mm, while the threaded length of the bolt was 50 mm. Figure 3 shows the details of the support and the reinforcement detailing.

2.3.2 Instrumentation

A total of 11 displacement transducers were used for each test: 1 for the slab deflection, measuring the vertical displacement from the bottom at the centre of the slab and 10 to detect crack openings. The location of the 10 gauges aimed at measuring crack openings is indicated in Fig. 4. For coding the instruments, COD (crack opening displacement) is followed first, by a subscript "t" if the instrument is placed on top of the slab or "b" if placed at the bottom of the slab, and then followed by a letter "L" for the two instruments with a longer gauge length. The last subscript shows the position of the instrument in the plane of the specimen with N standing for North, and W, S, and E standing for the other cardinal points. The nominal gauge length of each instrument is also given in Fig. 4. The instruments on top face of the slab were placed over the supports to capture possible negative cracking, and

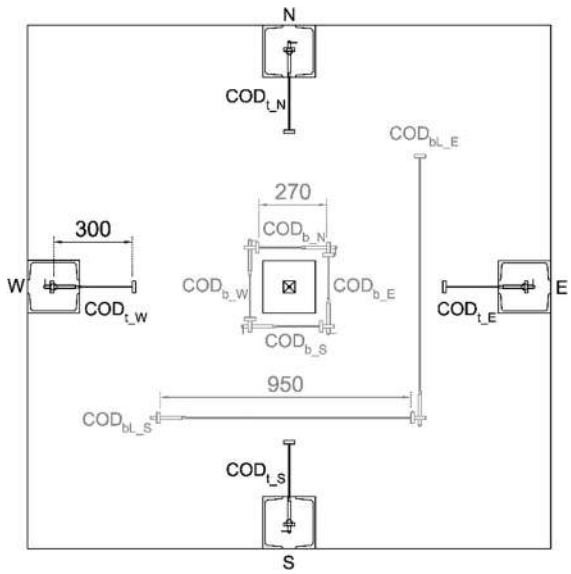

Fig. 4 Code and position of the ten instruments measuring crack opening: four at the top (black) and six at the bottom (grey)

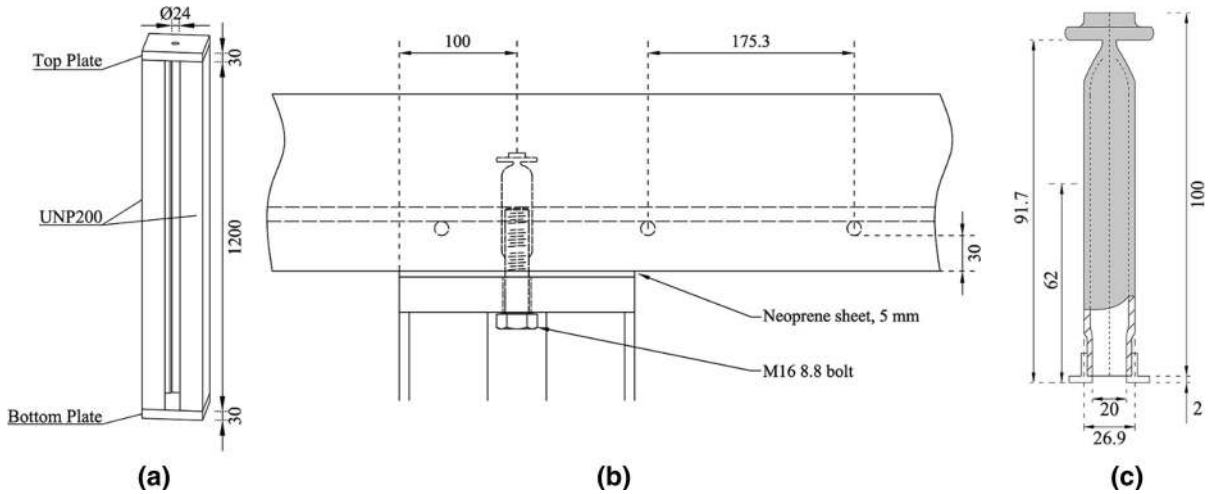

Fig. 3 Details of the support: **a** dimensions of the steel support; **b** details of the anchorage and reinforcement spacing; **c** drawing of the anchorage device

at the bottom of the slab four transducers were placed at 150 mm from the centre in a square configuration and those with a longer gauge length were placed at 500 mm from the centre. To measure the vertical deflection and the crack openings by instruments $COD_{bL\text{-}S}$ and $COD_{bL\text{-}E}$, potentiometer transducers were used, and the rest of the measurements were carried out by Linear Variable Deformation Transducers (LVDT).

3 Experimental results

3.1 Bending tests on notched beams

The nominal stress-CMOD curves for all fourteen specimens tested at different ages are shown in Fig. 5 and the statistical parameters obtained for flexural tensile strength, $f_{ct,fl}$, and post-peak residual strength values, $f_{R,1}$, $f_{R,2}$, $f_{R,3}$, and $f_{R,4}$ are reported in Table 1. The results are treated separately for specimens tested at 34 days and those tested at an older age. It is evident that there is a shift in material properties going from 34 to 167 and 220 days. While classifying the SFRC according to provisions of MC 2010 at 34 days leads to a "3c" material, taking into account the specimens tested at 167 and 220 days, a "5b" material is obtained. The use of a CEM IV cement may be a reason for the considerable strength increase with the curing time [40]. It is interesting to observe that even if the first cracking strength ($f_{ct,fl}$) increases for only 11%, the residual strength values of $f_{R,1}$ and $f_{R,2}$ (mainly related to SLS) experience a 30% increase of the average value. In case of larger CMOD values, less significant effects are observed: a 6% increase of $f_{R,3}$ average value and a slight decrease of 2.3% for $f_{R,4}$. Clearly, for the specimens tested in this study, age of the specimens has the most significant effect on strength values in the range of CMOD that corresponds to the SLS. Comparable observations were reported by Buttignol et al. [41], where SFRC specimens of 1 year and 10 years of age were tested in a four-point bending test. The results reported by the authors showed that there was a considerable increase in the peak and post-peak residual stresses up to a CMOD of 1 mm, while in the softening branch only a marginal strength increase was observed. In the present work, the coefficient of variation (CV) for $f_{R,1}$ and $f_{R,2}$ reduced with age while, for other strength values reported, the CV increased or did not change over time. Nevertheless, the CV falls approximately in the range of 15% to 20% for all the residual strength parameters and for both the groups.

In the MC 2010 two limitation are proposed for SFRC to be considered as a structural material, which are $f_{R1,k}/f_{ctk,fl} > 0.4$, and $f_{R3,k}/f_{R1,k} > 0.5$ to limit the brittleness in uniaxial tension behaviour guaranteeing

Table 1 Statistical parameters of the strength values obtained from the three-point bending test divided into two categories based on the testing age, in (MPa)

Group of specimens	f_{ct_fl}	$f_{R,1}$	$f_{R,2}$	$f_{R,3}$	$f_{R,4}$
34 (5 specimens)					
Mean	5.7	5.64	6.49	4.92	3.48
Std[a]	0.21	0.92	1.27	0.87	0.65
CV[b]	0.04	0.16	0.2	0.18	0.19
Charac-Normal[c]	5.21	3.48	3.54	2.88	1.96
Charac-LogN[d]	5.22	3.82	3.99	3.1	2.24
167 + 220 (9 specimens)					
Mean	6.32	7.36	8.73	5.2	3.39
Std	0.53	1.05	1.22	0.96	0.88
CV	0.08	0.14	0.14	0.18	0.26
Charac-Normal	5.28	5.3	6.34	3.32	1.67
Charac-LogN	5.34	5.39	6.48	3.5	1.97

[a]Standard deviation

[b]Coefficient of variation

[c]Characteristic value considering a normal distribution

[c]Characteristic value considering a log-normal distribution

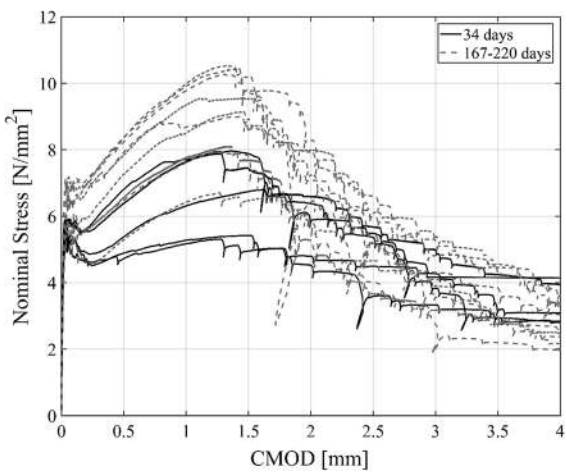

Fig. 5 Stress-CMOD results obtained from the bending tests

a minimum toughness in bending. Considering the results obtained here, over time the ratio of $f_{R,1k}/f_{ctk,fl}$ increased from 0.72 to 1 and the ratio $f_{R,3k}/f_{R,1k}$ reduced from 0.81 to 0.65. The latter indicates that over time, the same material tends to exhibit a less ductile behaviour in the post-peak range.

3.2 Slab test results

3.2.1 Load–deflection behaviour

The results obtained from the load–deflection behaviour of the slabs are shown in Fig. 6. Due to problems with recording the deflection data of RC1 specimen, the results of this test are not reported in this figure.

A quick glance at the deflection curve of the specimens reveals the substantial effect of steel fibres on the overall structural response of the elements. A major contribution of fibres is evident at approximately 120 kN, where R/C slabs undergo a sudden loss of stiffness. The stiffening effect brought by the steel fibres in the R/FRC slabs, leads to a stark difference between the deflection behaviour of the R/C and R/FRC slabs. After 200 kN, the deflection of the R/FRC slabs is less than half of the deflection of the R/C specimens. Even the slabs that are reinforced only with steel fibres show less deflection in this range of loading in comparison to the R/C slabs. It is worth noticing the very different deflection response of the R/C and R/FRC slabs reported in this study, and those reported in [19] where a four-point bending test was chosen to compare the behaviour of R/C and R/FRC slabs. Unlike the results presented here, the deflection of the R/FRC slabs, tested by Pujadas et al. was only slightly smaller than the R/C ones in the SLS range. This may be a clear indication of the superior efficiency of the application of fibres in redundant structural schemes, where higher stress redistribution coupled with multiple cracking may occur.

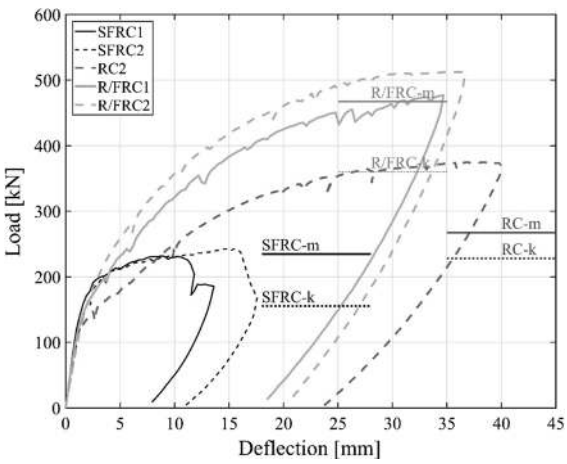

Fig. 6 Load-deflection results for the slabs tested and the ultimate load bearing capacity prediction obtained from yield line analysis based on average and characteristic material properties

The structural response of the SFRC specimens is characterized virtually by a bilinear behaviour. A first branch that goes up to around 190 kN for both of the specimens, and then a hardening behaviour controlled by the pull-out mechanism of the fibres. A 5% and 10% increase in the load level is observed for the SFRC1 and SFRC2 slabs during the hardening behaviour, before softening phase associated to crack localization occurs. The maximum load attained by the SFRC specimens is 232 kN and 243 kN at a deflection of 10.6 mm and 15.5 mm respectively for the SFRC1 and SFRC2 elements. Afterwards, a softening branch is observed and at a deflection of 13.5 mm for SFRC1 and 17.4 mm for SFRC2 the tests were stopped.

Steel fibres also largely affect the ultimate load bearing capacity of slab elements for elevated deflections if combined with conventional reinforcement. At a deflection of 35 mm the R/C specimens carry an average load of 365 kN, while the R/FRC companions sustain an average load of 494 kN which is 35% higher. The presence of fibres in the R/FRC specimens is responsible for an almost 130 kN of load difference between the R/C and R/FRC slabs.

3.2.2 Crack patterns

The final crack patterns for SFRC2, RC2, and R/FRC2 slabs are shown in Fig. 7. The cracks which appeared on the top of the slab elements are drawn with black lines, while the bottom cracks are marked with grey lines. The crack patterns show that there is a considerable difference in the extent of cracking between the SFRC slabs and those reinforced with rebars. Furthermore, the evolution of a circular crack on the top face of the R/C and R/FRC specimens is visible, which is a common mechanism for slab members under concentrated loading [42] if a boundary restraint is introduced. SFRC slabs are not capable of reaching the level of ductility required to activate the kinematic

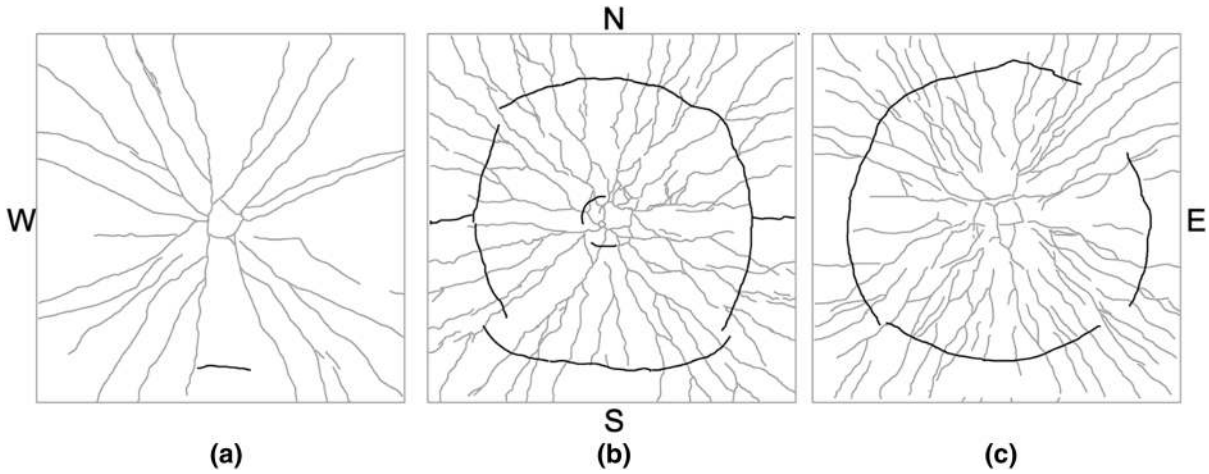

Fig. 7 Final crack patterns for **a** SFRC2, **b** RC2, and **c** R/FRC2 slabs. Bottom cracks are shown in grey and top cracks in black

mechanism of failure that comprises the cracking of the top surface of the slabs.

3.2.3 Bottom cracking

The results obtained from the instruments installed at the bottom of the specimens to capture the cracking behaviour, are shown in Figs. 8 and 9. Figure 8 illustrates the load-COD_b measurements and Fig. 9 concerns the COD_{bL} measurements. Due to technical problems the load-COD_{bL} curve for the RC1 specimen starts at a load of around 150 kN, which is marked by a circle on the figure. The COD values reported in Figs. 8 and 9a are the average values of the corresponding instruments. However, in order to examine the cracking behaviour of each slab in the two directions, Fig. 9b exhibits the load-COD_{bL} measurements carried out for specimens SFRC2, RC2, and R/FRC2 separately for both $COD_{bL\text{-}S}$ and $COD_{bL\text{-}E}$.

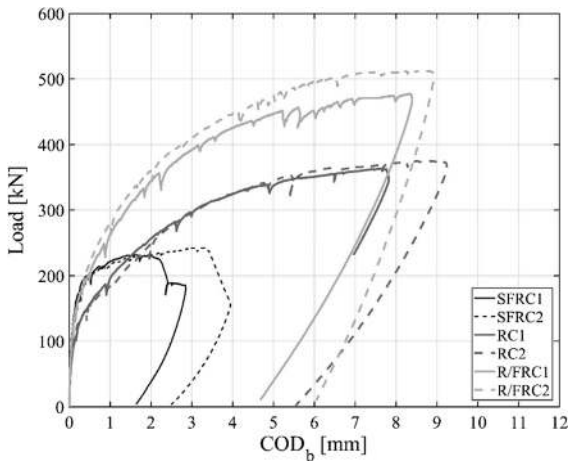

Fig. 8 The average Load-COD_b results measured by $COD_{b\text{-}N}$, $COD_{b\text{-}W}$, $COD_{b\text{-}S}$, and $COD_{b\text{-}E}$ instruments

Inspecting the bottom cracking behaviour of the slabs and zooming into the curves obtained, it can be noticed that the load-COD curves for RC1 and RC2 specimens diverge from those of the SFRC and R/FRC series at an earlier stage, as compared to the deflection response. The overall structural response of the slabs is less sensitive to the very local propagation of cracks. However, similar to the deflection behaviour, in the proximity of 120 kN, both COD_b and COD_{bL} measurements show a noticeable increase in the crack opening values. Looking at $COD_{bL\text{-}S}$ and $COD_{bL\text{-}E}$ measurements separately for SFRC2, RC2 and R/FRC2 slabs shown in Fig. 9b, it is observed that in each specimen the COD recorded by one of the instruments grows faster compared to the other one. In the results displayed for the three specimens, the crack opening measured by $COD_{bL\text{-}E}$ registers larger crack openings compared to $COD_{bL\text{-}S}$.

After 120 kN, in the SLS range, the effect of steel fibres in controlling the crack opening is easily recognized even without rebars. In the SFRC specimens the presence of steel fibres alone, leads to COD values that are half to one-third of the COD values measured in the R/C slabs and this observation holds until the point that the SFRC specimens go through an almost plastic deformation. The same comparison holds between the R/FRC and R/C elements.

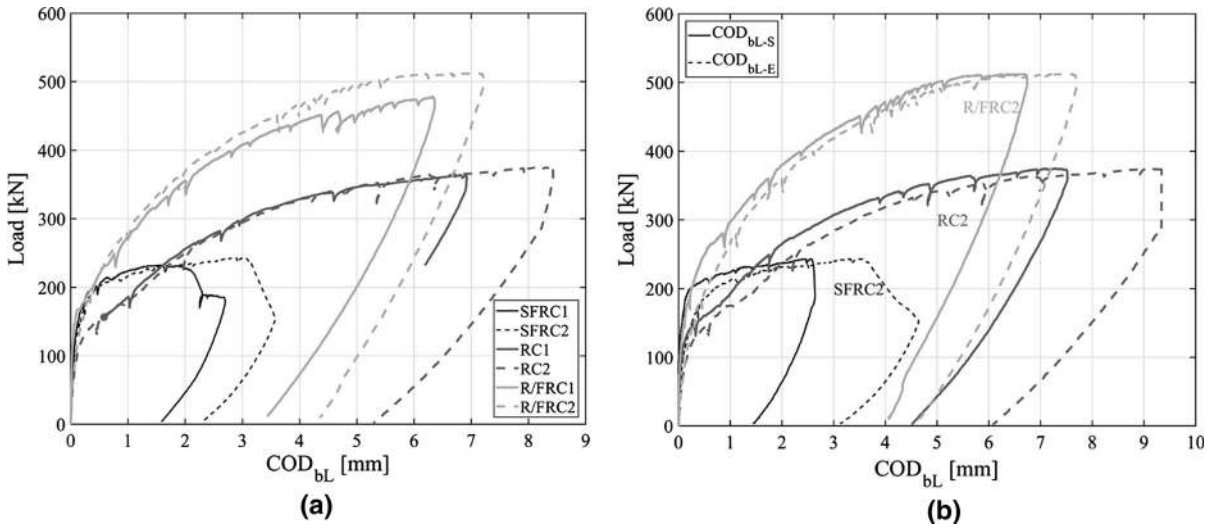

Fig. 9 SFRC2, RC2, and R/FRC2 specimens: **a** average Load-COD_{bL} results measured by COD_{bL-N}, COD_{bL-W}, COD_{bL-S}, and COD_{bL-E} instrument; **b** individual Load-COD_{bL} results measured by COD_{bL-S} and COD_{bL-E} instruments

For the SFRC slabs, although the two specimens are nominally identical, the COD values registered on COD_b and COD_{bL} measurements at the onset of the softening phase are different while comparable peak loads are obtained for these specimens. It is indeed pointed out that Figs. 8 and 9a are based on the average values of the measured CODs and they do not represent the measurement of a single instrument. Considering the recordings of each single COD_b measurement, it could be seen that for SFRC1 at maximum load, the reading of the four instruments vary between 1.45 and 2.55 mm and, soon after the softening behaviour, the instruments that pass over the localized crack start to register larger values, while other instruments register small variation in the COD. At the end of the test the COD_b measurements fall in the range of 1.66–4.22 mm for the SFRC1 slab. Comparable results are obtained for the SFRC2 slab. This is better shown in the Fig. 9b where for the SFRC2 specimen, as the softening phase unfolds, the COD_{bL-E} records increasing COD values associated to the localized crack, while the opening of the crack measured on COD_{bL-S} remains constant.

The significance of limiting crack widths to enhance durability of concrete structures cannot be overrated. There seems to be a crack width threshold below which the permeability of concrete is not affected. While according to Otieno et al. [43] this threshold depends on concrete mixture and properties, other studies mention a crack width approximately between 0.05 and 0.1 mm as the threshold [6, 44, 45]. At 0.05 mm of COD_b, the load carried by the SFRC and R/FRC slabs are 35% and 25% more than the load carried by the R/C slabs, and at 0.1 mm the difference is increased to almost 40% and 30%. The CODs reported are measured along the length of the instrument gauge and indicate the cumulative COD along the gauge. Therefore, there are chances that for the R/C and R/FRC slabs higher number of cracks with a narrower width would be recorded when compared to the SFRC slabs. Furthermore, the increased tortuosity of the crack surfaces in FRC mixtures may play a role in further reduction of cracked concrete permeability [46].

3.2.4 Top cracking

The results related to the cracking at the top surface of the slabs which are recorded at the position of the supports are presented in Fig. 10. The COD_t values are averaged between the number of instruments that have actually registered the propagation of a crack. The number shown on each curve gives the number of instruments that have passed over a crack.

According to these results it is evident that negative cracks develop only at late stages of loading. As mentioned earlier, the SFRC specimens do not experience negative cracking except for a short crack that

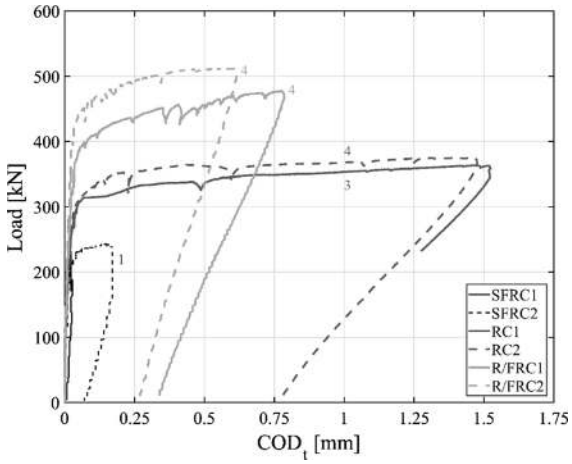

Fig. 10 Average load-COD_t results measured by $COD_{t\text{-}N}$, $COD_{t\text{-}W}$, $COD_{t\text{-}S}$, and $COD_{t,E}$ instruments. The number on each curve shows the number of instruments that have actually recorded the propagation of a crack

propagates at the position of $COD_{t\text{-}S}$ for SFRC2 slab. This crack opens up at 213 kN and reaches a COD of 0.17 mm at the end of the test. However, in case of specimens reinforced with rebars a complete circular negative crack pattern was developed.

The negative cracking for the R/C slabs starts to propagate at about 310 kN of load while for the R/FRC1 and R/FRC2 specimens the initiation of the negative cracks is respectively at 400 and 450 kN. Before stopping the test, the average COD_t measured for the R/C specimens are considerably larger than those measured for the R/FRC slabs. The effectiveness of steel fibres in controlling the opening of the negative moment cracks in the absence of top reinforcement is easily appreciated.

4 Discussion of results

Comparing the SFRC and R/C solutions in which 35 kg/m^3 and 70 kg/m^3 of steel is available respectivley, it is evident that twice the amount of steel weight in the R/C slabs with respect to the SFRC specimens, accounts for only a 55% increase in the load bearing capacity. It should also be noticed that the two layers of reinforcing steel are positioned exactly in the tensile region of the slabs, while the steel fibres are dispersed in the whole volume of the elements. Seemingly, the 3D spatial distribution of steel fibres leads to a more efficient stress distribution and consequently, a larger load bearing capacity when juxtaposed with the R/C companions.

Despite the efficiency in load carrying capacity, the shortcoming of the SFRC specimens is the lower ductility. At 10 and 15 mm of deflection, the SFRC slabs go through a softening phase, while the R/C ones continue on a plateau even at 40 mm of deflection. The limited ductility affects also the maximum load that is carried by the SFRC slabs. At a COD_b between 2 and 3 mm the softening phase is reached in these specimens, which prevents the activation of negative cracks thus also limiting the maximum load bearing capacity of the SFRC solution.

In the R/FRC slabs, the presence of rebars allow steel fibres to stay effective for a higher range of deformation. In these slabs at COD_b values of more than 8 mm, the effect of fibres is still present, and no major load reduction is observed. Hence, in the R/FRC slabs, not only the high ductility is assured, but the range of deflection in which the fibres are effective is increased. The effectiveness of fibres wears off at a certain crack opening when reached on a single crack. The diffused cracking due to presence of rebars, limits the COD on each single crack which in turn keeps the fibres active for larger deflection. Nevertheless, it is noticed that in terms of load carrying capacity, the interaction of steel fibres and rebars can not be fully uncoupled and the addition of the SFRC and R/C curves in the load direction does not yield the R/FRC curves.

The positive interaction between steel fibres and reinforcing rebars may be explained also considering the area below the load deflection curves. In Fig. 11,

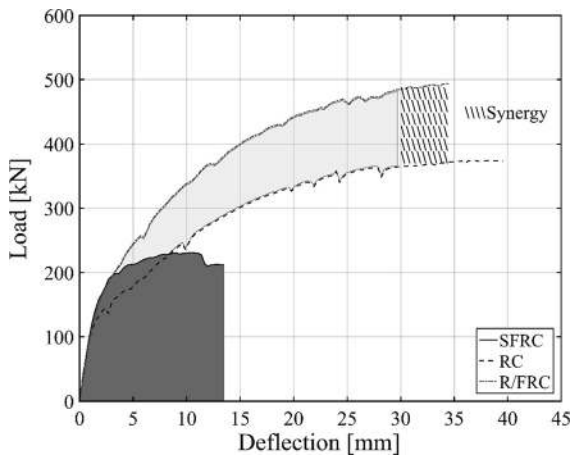

Fig. 11 Fibre/rebar synergic effect

the dark grey is the area under the load–deflection curve for the average behaviour of the SFRC elements, equal to 2.7 kNm, and the light grey depicts the same area, however filling the space between the load–deflection response of the R/FRC and R/C slabs, namely, the effect of fibres in R/FRC slabs. The curves are averaged up to the maximum deflection reached for the specimen that is unloaded at a smaller deflection. The hatched area, representing a 0.5 kNm of energy, is however, the additional energy that fibres provide in the R/FRC slabs as compared to the SFRC slabs. Hence, the presence of steel fibres in the R/FRC slabs is responsible for providing more energy compared to the effect of fibres in the SFRC specimens. While the topic of synergy between different types of fibres has been extensively studied [47–50], there seems to be also a synergetic effect in the fibre/rebar interaction. While in the present study the R/C and R/FRC specimens were unloaded just to avoid any possible damage to the instruments, it could be considered that the R/C and R/FRC slabs could have undergone higher levels of deflection, in which case the synergetic effect could have been better identified. It is worth to note that the negative bending moment activated along the top crack in the R/FRC slabs contributes to this effect.

5 Ultimate load prediction

A yield line approach is adopted to predict the ultimate load bearing capacity of the slab elements. Application of yield line method to fibre reinforced concrete slabs is a common practice which has been adopted elsewhere with satisfactory predictions of the ultimate load [51–53]. A yield line analysis considers an ultimate plastic behaviour for the material which is not the case for a SFRC material showing a softening behaviour. However, an almost plastic behaviour in the moment–curvature response allows for the implementation of this method to a softening material like the one investigated. The minimum ultimate load obtained according to a yield line configuration corresponds to a circular failure mechanism which agrees with the experimental crack pattern. The yield line pattern is shown in Fig. 12 and the ultimate load based on this failure mechanism is

$$P_u = 2\pi(m^+ + m^-) \quad (1)$$

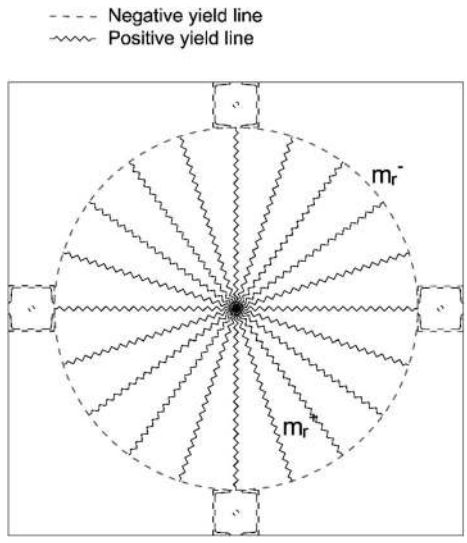

Fig. 12 Yield line mechanism adopted for the prediction of the ultimate load capacity

where m^+ and m^- are respectively positive and negative ultimate resistant bending moment. The computations are carried out once based on the mean values of material properties and once with the characteristic values both for steel and concrete. For the SFRC solution the material properties obtained from the tests carried out on 167 and 220 days are used, and a linear-elastic/linear-softening behaviour is adopted for the behaviour of fibre concrete in tension. To compute the sectional resisting bending moment a characteristic length equal to the thickness of the elements is chosen. No sedimentation effects were taken into account and therefore for the SFRC slabs a symmetric isotropic resistant bending moment is computed ($m^+ = m^-$). For the reinforcing bars, a plastic behaviour without hardening is first considered. The results obtained from the analysis for each slab type and for both cases, by assuming both the mean and the nominal characteristic material properties, are shown by a line segment in Fig. 6 and are respectively specified by a "m" and "k" letters. These values together with the experimental maximum loads and the design resisting loads obtained after introduction of proper partial safety factors are presented in Table 2. The predicted ultimate bearing capacity of the SFRC specimens using the mean values of material properties, almost exactly catches the ultimate experimental load, however, for the R/C slabs, given that the hardening of the reinforcement is not introduced in the

Table 2 Ultimate loads of investigated slabs: experimental, predicted and design values

	Maximum load (kN)			Design load (kN)
	Exp.	Predicted		
		Average	Characteristic	
SFRC	232/243	234	155	81
R/C	363/375	268	228	195
R/FRC	512/477	467	397	265

The redistribution factor considered for SFRC in Model Code 2010 (K_{Rd}) is set equal to 1

model, safe predictions are made for the maximum load. If the ultimate strength was taken into account, the ultimate load would increase for about 26%, growing from 268 to 314 kN.

Due to the specific boundary conditions chosen in the present study, negative moment cracks were not formed for the SFRC specimens. However, the ultimate limit state failure mechanism assumed comprises also cracks on the top surface of the slabs. Hence, while the ultimate load prediction for the SFRC slabs based on the complete circular fan gives a close prediction of the experimental maximum loads, the removal of the negative resisting moment in the formulation could have led to a significantly conservative prediction. This difference could be due to the lower CMOD in the slab test at the peak load when compared to the 2.5 mm considered as ultimate crack opening in the calculations. In fact the cumulative average COD_{bL} at the peak measured around 2–3 mm over more than 8 cracks, without any localization. Therefore, the actual stresses at the position of the cracks are closer to $f_{R,1}$ and $f_{R,2}$ values rather than the $f_{R,3}$ value which is introduced in the computations.

The fact that no negative cracks appeared on the top face of the SFRC slabs deserves more attention. Despite the lack of the negative cracking on the specimens, the introduction of the negative resisting moment in the ultimate load prediction gave satisfactory results for the present example, but it cannot be guaranteed as a rule. Therefore, the application of yield line kinematic approach according to limit analysis to compute the ultimate bearing capacity of FRC elevated slabs which may not show enough ductility to activate the complete failure mechanism may sacrifice safety of the overall structural behaviour. In this respect, provision of a minimum level of conventional reinforcing steel may well provide the required ductility. Finally, using the average material properties for the R/FRC slabs and considering the yield strength of rebars instead of the ultimate strength gives close prediction of the maximum experimental load. This indicates that the fibre contribution is reduced in this reinforcement solution.

In Table 2 also the design loads computed according to MC 2010, considering the redistribution coefficient K_{Rd} equal to the unity and starting from the nominal characteristic strengths of the materials, highlight the need to consider a proper value for this coefficient, mainly when no rebars are used, to balance the ratio between the experimental load and the predicted one.

6 Conclusions

In the present study the effect of application of steel fibres in a slab element with a statically redundant structural configuration under biaxial bending was investigated. Six concrete 2000 × 2000 × 150 mm solid slabs were tested under a concentrated load applied in the centre and measurements were carried out on deflection and cracking behaviour. Two slabs were reinforced with only steel fibres, two were reinforced with rebars and the last two slabs were reinforced with both the rebars and the steel fibres. The main conclusions derived from the present work are as follows.

- Utilization of 35 kg/m^3 of steel fibres for the SFRC slabs, and 35 kg/m^3 of reinforcing bars in each direction for the R/C slabs, allowed to make a comparison between the efficiency of the reinforcing solutions. Half the weight of steel in the SFRC

slabs as compared to the R/C ones, led to a peak load that was 64% of that obtained in the R/C specimens. The 3D distribution of fibres seems to be able to guarantee higher efficiency in terms of load bearing capacity in comparison with conventional rebars.

- SFRC slabs show limited ductility with respect to other reinforcing solutions. The lower ductility in the SFRC slabs may also affect the maximum load that is reached in these elements considering that the softening phase occurs before the appearance of negative moment cracks when a flexible constraint is considered. Provision of rebars is suggested to increase the deformation capacity of slabs.
- There is a positive interaction between steel fibres and reinforcing steel. In the R/FRC slabs, while the rebars guarantee the ductile behaviour of the slabs, the steel fibres remain active even under high levels of deflection giving their contribution also along the negative moment crack as assumed in the limit analysis. In this case the choice of the ultimate crack opening, set equal to 2.5 mm, allows to take into account the not contemporary contribution of positive and negative bending moment acting respectively on the radial and circumferential cracks.

Other observations made from the experiments and the prediction of the ultimate load based on the MC 2010 approach are as comes in the following lines:

- Stress-CMOD results obtained from the notched specimens show that while over time the residual tensile strength values in a range of CMODs that correspond to SLS improve, the residual strength for wider CMODs almost remains unchanged. This phenomenon may lead to a reduction of the ductility of SFRC structural elements that needs to be considered and further studied.
- Steel fibres are very effective in controlling deflection and cracking specifically in the SLS behaviour. In the range between 120 and 200 kN, the R/FRC slabs show 75% to 100% less deflection compared to the R/C specimens.
- A comparison between the negative moment cracks on the R/C and R/FRC slabs, shows that steel fibres can play a major role in reducing crack openings in the absence of a reinforcement layer on the top of the slabs.
- Following the approach suggested in *fib* MC 2010, and with the choice of the characteristic length equal to the depth of the slab, the ultimate load bearing capacity of the slabs is satisfactorily predicted by implementing a limit state analysis. Given the very high margin of safety between the design resisting load and the experimental maximum loads, the need of a redundancy factor as suggested by the Model Code for SFRC material contribution is proved in case of SFRC slabs.
- In order to apply a limit analysis to FRC elevated slabs characterized by a 3c class at 28 days, one should be assured about the possibility of the formation of the expected failure mechanism. Lower ductility of SFRC slabs without any rebars might not allow the complete formation of the expected kinematic failure mechanism which could lead to unsafe prediction for the ultimate load.

Acknowledgements The authors express their gratitude to the financial support provided by Steriline, Magnetti Building, and Finazzi Company and the technical support provided by DSC-Erba. The authors are also grateful to the assistance of Mr. Andrea G. Stefanoni for his contribution in carrying out the experiments.

Compliance with ethical standards

Conflict of interest The authors declare that they have no conflict of interest.

References

1. Romualdi JP, Batson GB (1963) Behaviour of reinforced concrete beams with closely spaced reinforcement. ACI J Proc 60(6):775–790
2. Shah S, Rangan B (1971) Fibre reinforced concrete properties. ACI J Proc 68:126–137
3. Rossi P, Chanvillard G (2000) PRO 15: 5th RILEM symposium on fibre-reinforced concretes (FRC)-BEFIB'2000, vol 15. RILEM Publications, Cachan
4. di Prisco M, Felicetti R, Plizzari GA (2004) PRO 039: 6th international RILEM symposium on fibre-reinforced concretes BEFIB'2004. RILEM Publications, Cachan

5. Gettu R (2008) PRO 060: 7th international RILEM symposium on fibre reinforced concrete: design and applications—BEFIB'2008. RILEM Publications, Cachan
6. Naaman AE (1998) New fiber technology. Concr Int 20(7):57–62
7. Wang K, Jansen DC, Shah SP, Karr AF (1997) Permeability study of cracked concrete. Cem Concr Res 27(3):381–393
8. Bischoff PH (2003) Tension stiffening and cracking of steel fibre reinforced concrete. J Mater Civ Eng 15(2):174–182
9. Abrishami HH, Mitchell D (1997) Influence of steel fibres on tension stiffening. ACI Struct J 94(6):769–776
10. Tiberti G, Minelli F, Plizzari GA, Vecchio FJ (2014) Influence of concrete strength on crack development in SFRC members. Cem Concr Compos 45:176–185
11. Deluce JR, Seong-Cheol L, Vecchio FJ (2014) Crack model for steel fibre-reinforced concrete members containing conventional reinforcement. ACI Struct J 111(1):93–102
12. Heek P, Mark P (2014) Load-bearing capacities of SFRC elements accounting for tension stiffening with modified moment-curvature relations, pp 301–310
13. Meda A, Minelli F, Plizzari GA (2012) Flexural behaviour of R/C beams in fibre reinforced concrete. Compos Part B Eng 43(8):2930–2937
14. Oh BH (1992) Flexural analysis of reinforced concrete beams containing steel fibres. J Struct Eng 118(10):2821–2835
15. Alsayed SH (1993) Flexural deflection of reinforced fibrous concrete beams. ACI Struct J 90(1):72–88
16. Vandewalle L (2000) Cracking behaviour of concrete beams reinforced with a combination of ordinary reinforcement and steel fibres. Mater Struct 33(3):164–170
17. Tan KH, Paramasivam P, Tan KC (1995) Cracking characteristics of reinforced steel fibre concrete beams under short- and long-term loadings. Adv Cem Based Mater 2(4):127–137
18. Mertol HC, Baran E, Bello HJ (2015) Flexural behaviour of lightly and heavily reinforced steel fibre concrete beams. Constr Build Mater 98:185–193
19. Pujadas P, Blanco A, De La Fuente A, Aguado A (2012) Cracking behaviour of FRC slabs with traditional reinforcement. Mater Struct Constr 45(5):707–725
20. Dossland AL (2008) Fibre reinforcement in load carrying concrete structures. PhD Thesis, Norvegian University of Science and Technology, Norway, Trondheim
21. di Prisco M, Plizzari G, Vandewalle L (2009) Fibre reinforced concrete: new design perspectives. Mater Struct 42(9):1261–1281
22. Mobasher B, Destrée X (2010) Report on design and construction of steel fibre-reinforced concrete elevated slabs. In: SP-274 fibre reinforced self-consolidating concrete: research and applications
23. Facconi L, Minelli F, Plizzari G (2016) Steel fibre reinforced self-compacting concrete thin slabs—experimental study and verification against Model Code 2010 provisions. Eng Struct 122:226–237
24. Fall D, Shu J, Rempling R, Lundgren K, Zandi K (2014) Two-way slabs: experimental investigation of load redistributions in steel fibre reinforced concrete. Eng Struct 80:61–74
25. Fédération internationale du béton (2013) Model code 2010: final draft. International Federation for Structural Concrete (fib), Lausanne
26. Roesler JR, Lange DA, Altoubat SA, Rieder K-A, Ulreich GR (2004) Fracture of plain and fibre-reinforced concrete slabs under monotonic loading. J Mater Civ Eng 16(5):452–460
27. Sorelli LG, Meda A, Plizzari GA (2006) Steel fibre concrete slabs on ground: a structural matter. ACI Struct J 103(4):551–558
28. Falkner H, Henke V (1998) Application of steel fibre concrete for underwater concrete slabs. Cem Concr Compos 20(5):377–385
29. Destrée X, Mandl J (2008) Steel fibre only reinforced concrete in free suspended elevated slabs: case studies, design assisted by testing route, comparison to the latest SFRC standard documents. Proceedings of Tailor Made Concrete Structures - New Solutions for our society. Taylor & Francis Group, London, p 437–443
30. Hedebratt J, Silfwerbrand J (2014) Full-scale test of a pile supported steel fibre concrete slab. Mater Struct Constr 47(4):647–666
31. di Prisco M, Martinelli P, Parmentier B (2016) On the reliability of the design approach for FRC structures according to fib Model Code 2010: the case of elevated slabs. Struct Concr 17(4):588–602
32. Parmentier B, Van Itterbeeck P, Skowron A (2014) The flexural behaviour of SFRC flat slabs: the Limelette full-scale experiments for supporting design model codes. Proceedings of FRC 2014 Joint ACI-fib International Workshop
33. di Prisco M, Sibaud F, Failla C, Finazzi P, Siboni A, Bassani A, Nava G, Colombo M (2018) Innovative SFRC applications: an industrial building in Como. In: Proceedings of *Italian concrete days*, June 14–15, Lecco. ISBN: 978-88-99916-11-4
34. EN 14651 (2005) Test method for metallic fibreed concrete—measuring the flexural tensile strength (limit of proportionality (LOP), residual). European Commission Standard, Brussels
35. Blanco A, Pujadas P, De La Fuente A, Cavalaro SHP, Aguado A (2015) Assessment of the fibre orientation factor in SFRC slabs. Compos Part B Eng 68:343–354
36. Barnett SJ, Lataste J-F, Parry T, Millard SG, Soutsos MN (2010) Assessment of fibre orientation in ultra high performance fibre reinforced concrete and its effect on flexural strength. Mater Struct 43(7):1009–1023
37. Pujadas P et al (2014) Plastic fibres as the only reinforcement for flat suspended slabs: parametric study and design considerations. Constr Build Mater 70:88–96
38. Zhou B, Uchida Y (2017) Relationship between fibre orientation/distribution and post-cracking behaviour in ultra-high-performance fibre-reinforced concrete (UHPFRC). Cem Concr Compos 83:66–75
39. Soroushian P, Lee CD (1990) Distribution and orientation of fibres in steel fibre reinforced concrete. ACI Mater J 87(5):433–439
40. Neville A (1995) Properties of concrete. Longman, London
41. Buttignol TET, Colombo M, di Prisco M (2016) Long-term aging effects on tensile characterization of steel fibre reinforced concrete. Struct Concr 17(6):1082–1093
42. Park R, Gamble WL (2000) Reinforced concrete slabs. Wiley, New York
43. Otieno M, Alexander MG, Beushausen H-D (2010) Corrosion in cracked and uncracked concrete—influence of crack

width, concrete quality and crack reopening. Mag Concr Res 62(6):393–404
44. Rapoport J, Aldea C-M, Shah SP, Ankenman B, Karr A (2002) Permeability of cracked steel fibre-reinforced concrete. J Mater Civ Eng 14:355–358
45. Berrocal CG, Löfgren I, Lundgren K, Tang L (2015) Corrosion initiation in cracked fibre reinforced concrete: influence of crack width, fibre type and loading conditions. Corros Sci 98:128–139
46. Berrocal CG, Löfgren I, Lundgren K, Görander N, Halldén C (2016) Characterisation of bending cracks in R/FRC using image analysis. Cem Concr Res 90:104–116
47. Banthia N, Gupta R (2004) Hybrid fibre reinforced concrete (HyFRC): fibre synergy in high strength matrices. Mater Struct 37:707–716
48. Park SH, Kim DJ, Ryu GS, Koh KT (2012) Tensile behaviour of ultra high performance hybrid fibre reinforced concrete. Cem Concr Compos 34:172–184
49. Kim DJ, Park SH, Ryu GS, Koh KT (2011) Comparative flexural behaviour of hybrid ultra high performance fibre reinforced concrete with different macro fibres. Constr Build Mater 25:4144–4155
50. Sorelli LG, Meda A, Plizzari GA (2005) Bending and uniaxial tensile tests on concrete reinforced with hybrid steel fibres. J Mater Civ Eng 17(5):519–527
51. Salehian H, Barros JAO, Taheri M (2014) Evaluation of the influence of post-cracking response of steel fibre reinforced concrete (SFRC) on load carrying capacity of SFRC panels. Constr Build Mater 73:289–304
52. Kleinman C, Destrée X, Lambrechts A, Hoekstra A (2012) Steel fibre as only reinforcing in free suspended one way elevated slabs: design conclusions of a Tu, pp 1–13
53. Colombo M, Martinelli P, di Prisco M (2017) On the evaluation of the structural redistribution factor in FRC design: a yield line approach. Mater Struct 50(1):100